PROTON IRRADIATION EFFECTS IN MOS AND JUNCTION FIELD-EFFECT TRANSISTORS AND INTEGRATED CIRCUITS

By Floyd R. Eryant, Carl L. Fales, Jr.,
and Roger A. Breckenridge

NASA Langley Research Center
Langley Station, Hampton, Va.

Presented at the Fifth Annual Symposium on the
Physics of Failure

Columbus Ohio
November 15-17, 1966

ABSTRACT

Because of the application of field-effect transistors, and integrated circuits in space electronic systems and the fact that proton irradiation data at energies typical of a space environment are not extensive, an experimental evaluation of these devices has been conducted. The important electrical parameters of these devices were measured before, during, and after irradiation at the Oak Ridge National Laboratory's 22-MeV cyclotron.

The results obtained from the MOS field-effect study show that their degradation processes include that of charge storage in the silicon dioxide insulating layer and radiation-induced changes in surface states. MOS transistors have been found to degrade at orders of magnitude less integrated proton flux than many bipolar and junction field-effect transistors; therefore, for space applications in radiation fields such as Van Allen Belts and solar particle events, these devices may be subject to serious radiation damage.

The junction field-effect transistor displays a large initial spread in device irradiation response. However, it appears to possess a high degree of resistance to proton irradiation.

The integrated circuits tested were of the monolithic type and under proton irradiation displayed a large reduction

of minority carrier lifetime in the base region of the circuit transistors. Other less important defects are reduction of free carrier concentration and reduction in mobility. Important electrical parameters that are affected by radiation are input threshold voltages, output low level voltages, leakage currents, and transient characteristics.

In conclusion, MOS field-effect transistors and integrated circuits display significant damage characteristics when subjected to a space proton environment. It is important that these effects be considered when electronic circuits are to be subjected to a space radiation environment.

INTRODUCTION

Metal-oxide-semiconductor and junction field-effect transistors and integrated circuits are three electronic devices which have characteristics that make them attractive for space applications. The MOS-FET's provide ultrahigh input impedance, wide choice of bias polarities for complementary logic circuitry, and good compatibility with microelectronic or integrated circuit technology. The junction FET's possess high input impedance and low noise characteristics. Both FET's are voltage amplifiers as contrasted to bipolar transistors which are current amplifiers. Silicon integrated circuits provide small size and weight, low power requirements, and high reliability.

The effects of the space radiation environment on the performance of these devices must be established before they can be used with confidence in space electronic systems. From a radiation damage point of view, junction and MOS-FET's, which are majority carrier devices, would be expected to possess a greater resistance to radiation than bipolar transistors, which are minority carrier devices. These expectations have been substantiated for the junction FET by work at the NASA Langley Research Center[1]; however, results reported elsewhere[2] indicate the MOS devices may be as susceptible to damage as conventional bipolar transistors.

Since most silicon integrated circuits employ bipolar transistors, it would be expected that their radiation damage would be dominated by the damage experienced by the individual transistors. The complex nature of the circuits, the various coupling schemes, and differences in manufacturing techniques, however, increase the difficulty in predicting their response to radiation.

Since data on proton irradiation effects in these three devices [illegible] extensive, experimental studies were conducted by the NASA Langley Research Center at the Oak Ridge National Laboratory's 22-MeV cyclotron. Small groups of junction and MOS-FET's and integrated circuits were irradiated and changes in critical electrical parameters measured. Analyses were performed to provide some insight into the cause of the observed damage in each device. This paper reports the results of this investigation.

EXPERIMENTAL PROCEDURE

The three devices discussed in this report were bombarded with 22-MeV protons at the Oak Ridge National Laboratory 86-inch cyclotron. The beam uniformity was improved by passing it through a scattering foil and a one-half-inch-diameter collimator. The beam current was monitored with a specially designed thin window ion chamber which had been calibrated with a Faraday cup. A current integrator monitored the ion chamber current giving a direct measure of integrated flux. The proton flux rate for these experiments was about 10^9 protons/cm^2/sec.

Measurements of the critical electrical parameters were made before and after irradiation, and the devices were maintained at room temperature during irradiation. Details of a typical experimental setup are described in reference 1.

RESULTS AND DISCUSSION

Junction Field-Effect Transistors

Test results for the silicon junction field-effect transistors are briefly summarized in table I. The table gives the integrated proton flux range necessary to cause 30-percent degradation to zero gate drain current, I_{DSS}, and zero gate transconductance, g_{mo}, for the FET's after bombardment by 22-MeV protons. Thirty-percent degradation was not always achieved and the exceptions are noted in the table.

TABLE I. BRIEF SUMMARY OF 22-MeV PROTON IRRADIATIONS

Transistor type	Proton flux necessary to cause 30% degradation in I_{DSS}, protons/cm^2	Degradation at indicated flux, %	Proton flux necessary to cause 30% degradation in g_m, protons/cm^2	Degradation at indicated flux, %
2N3067	$3.4 \pm 1.6 \times 10^{12}$	30	$4.5 \pm 2.5 \times 10^{12}$	30
2N3386	8×10^{12}	10 to 30	7×10^{12}	5 to 20
2N2344	$3.5 \pm 1.5 \times 10^{12}$	30	$5.3 \pm 1.8 \times 10^{12}$	30
2N3089	$5.0 \pm 3.0 \times 10^{12}$	30	$4 \pm 3 \times 10^{12}$	30
2N3070	$5.8 \pm 2.3 \times 10^{12}$	30	$5.8 \pm 2.1 \times 10^{12}$	30
2N3086	$6.6 \pm 1.4 \times 10^{12}$	12 to 16	8×10^{12}	8 to 12
2N3088	$5.0 \pm 2.0 \times 10^{12}$	30	$5.5 \pm 2.5 \times 10^{12}$	30
2N2497	$2.3 \pm 1.0 \times 10^{13}$	30	$5.3 \pm 0.2 \times 10^{13}$	30
2N3085	2×10^{13}	10 to 15	2×10^{13}	7 to 14

Comparison of the above data with that of reference 2 indicates that the radiation resistance of junction FET's is at least comparable to or better than most narrow-base minority carrier devices.

Spread exists among the responses of the transistors of a particular type to the damaging radiation. One cause of the transistor response variations, which results in radiation response scatter noted in many of the FET's, originates from unwanted impurities remaining in the semiconductor material after fabrication. The

damage to the crystal (carrier removal rate) is sensitive to these impurities.

Three transistor types from the above table were examined in sufficient detail to study the variation of drain current and transconductance as functions of integrated proton flux based on a carrier removal rate model. The expressions of drain current and transconductance for the junction field-effect transistor are more readily amenable to analysis if the gate to source voltage is maintained at a zero level. Two physical models[3,4,5] state that the zero gate voltage drain current, I_{DSS}, is proportional to the carrier mobility, μ, and varies as the square of the carrier concentration. The zero gate voltage transconductance, g_{mo}, varies as the product of mobility and carrier concentration. These simplified zero gate voltage equations are

$$I_{DSS} = C_1 \mu n^2, \quad g_{mo} = C_2 \mu n. \tag{1}$$

Certain assumptions must still be made about the displacement particle dependence of carrier mobility and concentration.

The semipermanent damage induced in the bulk of a semiconductor is in the form of lattice defects caused by the displacement of atoms within the crystal. These defects introduce energy levels in the forbidden gap of the semiconductor which behave as donor and acceptor states and recombination centers. Allowed energy levels in the forbidden energy gap will alter the mobile carrier concentration and, depending on their charge state, function as scattering centers reducing the carrier mobility.

A semiempirical relation[6,7,8] between carrier concentration (or carrier charge density) and energetic particle flux is given by

$$n = n_o + (dn/d\phi)_o \phi \tag{2}$$

where n_o = initial carrier concentration

ϕ = integrated particle flux

$(dn/d\phi)_o$ = initial carrier removal rate.

The following restrictions are assumed: (1) the Fermi level does not change its position in the forbidden energy gap as the concentration of donor and acceptor defect levels increases and (2) the semiconductor material is sufficiently thin that the energy of the assumed monoenergetic radiation does not significantly degrade in passing through since $(dn/d\phi)_o$ is energy dependent.

However, the Fermi level will begin to shift under extended particle bombardment with the changing conductivity in such a way to decrease the fractional filling of the pertinent acceptors or donors. The carrier concentration then drops less rapidly than equation (2)

indicates. The linear dependence of carrier concentration on flux appears to hold well until conductivities reach one-half their initial values.

Since the carrier mobility degradation is usually small compared to carrier concentration decreases, equation (2) can be combined with equation (1) to yield the particle flux dependence of the zero gate voltage drain current and transconductance

$$I_{DSS} = I_{DSS_o}(1 + \gamma\phi)^2 \tag{3}$$

$$g_{mo} = g_{mo_o}(1 + \gamma\phi), \tag{4}$$

where $\gamma = 1/n_o(dn/d\phi)_o$.

Since it is expected that g_{mo} should more closely follow a linear variation with flux than does drain current, a best linear fit under least squares is first applied to the g_{mo} versus ϕ data. Types 2N3070 and 2N2844 possess g_{mo} variations in reasonable accord with the anticipated first-degree dependence. Unexpectedly, the drain current versus ϕ data of type 2N3067 also adapts to a straight-line fit. The results are

$$g_{mo}/g_{mo_o} = (1 - 0.148 \times 10^{-13}\phi) \text{ - type 2N3070} \tag{5}$$

$$g_{mo}/g_{mo_o} = 0.986(1 - 0.0737 \times 10^{-13}\phi) \text{ - type 2N2844} \tag{6}$$

$$I_{DSS}/I_{DSS_o} = 1.003(1 - 0.1859 \times 10^{-13}\phi) \text{ - type 2N3067} \tag{7}$$

where ϕ is in the units, protons/cm^2. These equations are plotted as solid lines in figures 1, 2, and 3.

The numerical coefficients of flux in the above linear equations can be directly related to initial carrier removal rate. Thus, without recourse to any device specifications, a rough comparison may be made between material and device carrier removal rates. For the proton energy pertinent here, average initial carrier removal rates of -7.6 and -13 for 10Ω-cm n- and p-type silicon, respectively, have been observed. From equations (5) and (6), the corresponding device rates for types 2N3070 (n-channel) and 2N2844 (p-channel) are both -7.4 in reasonable agreement with the 10Ω-cm silicon.

Equations (3) and (4) indicate a square law dependence of drain current on transconductance for the parametric variable, ϕ, given by

$$I_{DSS}(\phi)/I_{DSS_o} = \left[g_{mo}(\phi)/g_{mo_o}\right]^2.$$

Figure 4 shows logarithmic plots of transconductance as a function of drain current for the transistor types. The solid lines correspond to the most probable linear adaptation of the data in the logarithmic scale. Good statistical agreement holds for type 2N3070 and to a lesser extent in types 2N2844 and 2N3067. The slopes of these curves are:

$\beta = 1.27$ - type 2N3070

$\beta = 1.60$ - type 2N2844

$\beta = 1.35$ - type 2N3067.

Therefore, it is found that the exponent, 2, must be replaced with an arbitrary constant to preserve the power law nature of the I_{DSS} and g_{mo} relationship which may be represented as

$$I_{DSS}(\phi)/I_{DSS_o} = \alpha\left[g_{mo}(\phi)/g_{mo_o}\right]^{\beta},$$

where β seems to satisfy the inequality $1 < \beta < 2$ and α is near unity.

MOS Field-Effect Transistors

The several examples of the 22-MeV proton irradiations which follow are not given as statistical averages of large numbers of devices of the same type but rather single cases exemplary of the different or contrasting behavior encountered. Among these are both experimental and commercially available transistors.

P-Channel Enhancement Units

Since p-channel enhancement-type MOS structures, whose characteristics depend only slightly on carrier concentration, are found to be more sensitive to radiation than most bipolar devices,[2] we shall focus first on the experimental findings for this transistor.

Figure 5 shows a plot of pinch-off voltage as a function of integrated proton flux (22 MeV) for a p-channel enhancement device possessing an initial $V_p = -1.2$ volts. The pinch-off voltage was obtained by measuring the small signal conductance between the source and drain for a range of gate-source voltages. The pinch-off voltage increases negatively quite rapidly in the early stages of bombardment. For increasing integrated flux the rate of degradation decreases, and the rate tends to a constant value. This behavior is similar to the neutron results of Messenger et al.[9]

A convenient schematic way of discussing this behavior is to examine figure 6 which shows an energy band diagram of the MOS structure in thermal equilibrium (no applied biases) prior to irradiation. This gives a qualitative picture of a practical p-channel enhancement transistor. The silicon-dioxide layer is assumed to be

equivalent to the vacuum (SiO_2 is not crystalline and exhibits no energy band properties in the usual sense). Here, ρ_o is assumed to be a homogeneous charge distribution in the SiO_2 layer as a result of the ionizing and displacement producing radiation, and σ_{ss} is the net surface states charge density which is dependent on the relative location of the Fermi potential to the electrostatic potential of the surface, $\psi_s - \phi$. For present purposes σ_{ss} is assumed constant.

The pinch-off or turn-on condition is that point at which the net space charge region ceases to extend to the surface and an inversion layer of opposite conductivity to that of the substrate begins to form. For open circuit source and drain, a straightforward procedure in solving Poisson's equation combined with the appropriate boundary conditions leads to an approximate expression for the pinch-off voltage

$$V_P = -C_3\rho_o - C_4\sigma_{ss} + f\left(\left|N_D^+ - N_A^-\right|\right), \tag{8}$$

where C_3 and $C_4 > 0$ and $f\left(\left|N_D^+ - N_A^-\right|\right)$ is a function of the net ionized donor and acceptor charge density.

The second term in equation (8) indicates that the pinch-off voltage is proportional to the surface charge (σ_{ss}) and takes on negative values for a positive charge density. The proton bombardments can effect changes in the number of surface states and a redistribution in their densities as a function of energy in the forbidden gap. An exaggerated example is given in the plot of density of states versus energy given in figure 7. Comparing this distribution with the unirradiated density distribution, notice the increased area under the density curve corresponding to a greater number of states and the reshaping of the density leading to peaks at different energies. As shown in the figure, there are more states with energies above the Fermi level than the unirradiated case. This leads to a greater positive surface charge and more pronounced bending of the bands and finally a negative increase in pinch-off voltage.

Another and perhaps the most important mechanism contributing to the pinch-off voltage is the presence of mobile ions (temperature dependent concentration and mobility) in the SiO_2 layer. These ions are reasoned[10] to be negatively charged oxygen ions. They are disassociated thermally from the oxide thus leaving a positively charged oxygen vacancy site. The presence of a reducing agent such as the metal of the gate electrode can remove some of the oxygen ions thus disturbing the stoichiometric ratio of the SiO_2, substantially increasing the ion mobility, and finally resulting in a net diffusion of the ions. This process may leave a net positive charge density of oxygen vacancies in the oxide as shown in figure 6. Electric fields in the oxide also contribute to the effect. It is interesting to note that no negative charge density in SiO_2 has been observed. A net positive distribution of such ions in the oxide can cause a further negative increase in V_P as seen from the first

term of equation (8). These ions in the oxide give rise to many of the temperature, biasing, and aging instabilities in the MOS devices.

Messenger et al.[9] have studied the change in pinch-off voltage in p-channel enhancement devices under nonionizing neutron bombardments. They observed a net positive charge density in the dielectric and set forth a tentative hypothesis that oxygen vacancies produced by displacement are formed in the SiO_2. These are the same type positive ions mentioned previously which were excited thermally rather than by neutron collisions.

Twenty-two MeV protons should generally have a greater cross section for displacement scattering than the reactor neutrons. We thus expect that the effects of displacements in the oxide will be significant for the proton irradiations. Taking the positive charge density hypothesis as the predominant damage mechanism,[9] the characteristic asymptotic appearence of V_P as a function of integrated flux is explained from two assumptions: (1) that the number of positive charge centers created is proportional to integrated flux and (2) the positive charge centers disappear via recombination or diffusion during the irradiation at a rate proportional to their density.

A positive charge density in the dielectric, which would be proportional to proton flux at small doses, gives rise to the steep rate of change of V_P (fig. 5). The leveling or saturation effect at greater doses may well result from the rate of recombination or diffusion of the proposed oxygen vacancies which is proportional to the charge density present in the oxide at a given instant. Finally, the rather constant rate of negative increase observed at extended integrated flux levels can be associated with the carrier concentration dependence of the third term of equation (8) for V_P.

The plausibility of the shape of figure 5 has been discussed without mention of the second term of equation (8) which varies as the net surface states charge density. The surface states energy distribution and number are sensitive to the proton radiation. A saturation or steady state radiation environment configuration for the surface states is also possible leading again to a constant value of σ_{ss} and a degradation rate decrease.

Figure 8 gives a plot of normalized drain current as a function of integrated flux for an experimental p-channel enhancement unit possessing an initial pinch-off voltage of approximately -4 volts. These curves are interesting primarily because the drain current is a more direct terminal electrical characteristic of the transistor which in turn is dependent on pinch-off voltage and carrier mobility[10] from

$$I_D = -C_5 \mu_p (V_{GS} - V_P)^2. \qquad (9)$$

Notice the rapid degradation rate of drain current in figure 8. This MOS transistor is probably worthless as a circuit component at 5×10^{10} protons/cm^2 (a relatively low flux).

Figure 9 is a plot of the transfer characteristics for the same experimental transistor for the preirradiation condition, $\phi = 10^{11}$ protons/cm^2, $\phi = 2(10)^{12}$ protons/cm^2, and 2 months after irradiation at room temperature under no biases. All curves appear roughly square law (eq. (9)). Graphically, we find that $V_P \approx -4$, -5.5, and -8 volts for the integrated fluxes $\phi = 0$, 1×10^{11}, and 2×10^{12} protons/cm^2, respectively. The three curves possess very similar slopes, where the slope is the transconductance[11] (eq. (10)) and differ in the horizontal translation of their axes.

$$g_m = -2C_5\mu_p(V_{GS} - V_P) \qquad (10)$$

This implies that changes in mobility are small relative to pinch-off degradation as expected.

The curve for 2 months after irradiation has a slightly increased slope contrary to what we know about the small decrease in mobility and exhibits some annealing of pinch-off voltage to $V_P = -7.3V$. The anneal direction of the pinch-off voltage is expected although somewhat small in magnitude. This extent of room temperature annealing may correspond to the small rate of recombination or diffusion of the positive ions when the oxide is not being exposed to the radiation field.

Experimental evidence[10] indicates that, during annealing at elevated temperatures, the pinch-off voltage for MOS structures with a pure SiO_2 layer is very sensitive to the magnitude and polarity of bias voltages applied across the oxide. For both p- and n-type silicon substrates, the pinch-off voltage takes on sizable negative values (much larger than the bias potential) when the gate is positive relative to the silicon. In contrast, under negative gate bias V_P will change to a lesser extent but in the opposite direction toward a less negative value. These observations are explained by the hypothesis that the oxygen ion motion is enhanced by the applied electric field. For p-channel enhancement operation, increasing negative gate bias should result in a decreased rate of change for V_P. Contrary to this, it has been observed, in the 22-MeV proton experiments and in the results of H. E. Wannamacher (Goddard Space Flight Center, unpublished paper), that the rate of negative increase in V_P is significantly increased due to negative biases during irradiation. This behavior can be explained by a more detailed model, which accounts for the diffusion of phosphorus into the oxide to improve temperature and bias stabilities.

N-Channel Units

Figure 10 shows a plot of normalized drain current versus integrated proton flux at several values of gate-source voltage for

an n-channel depletion transistor. Notice that for very early fluxes the drain current more than doubles in magnitude, reaches a maximum, and begins slow descent to a value less than the initial one. We attribute the rapid buildup of drain current to the much discussed net positive charge density (including oxygen vacancies) in the oxide which induces correspondingly more electrons in the channel and leads to a more negative value of pinch-off voltage.

The phenomena leading to the reduction rate may have several origins. These include: (1) The recombination rate (discussed earlier) of the oxygen ions and oxygen vacancies increases sufficiently to give a leveling off of drain current (and Vp) which was expected in the experimental curves. This limits the increase in saturation drain current but cannot alone account for net decrease in I_D. (2) The oxide could lose its ability to support the charge density if electric fields became strong. (3) Degradation in carrier mobility occurs at these fluxes but is still small, say less than 10 percent in the 10^{12} protons/cm^2 range. (4) A conditioning of the oxide under the combined influence of the proton flux and the negative gate bias possibly took place giving a permanently lower magnitude of pinch-off voltage than the initial value (room temperature annealing is discussed shortly). A closer tie-in with the model for the p-channel device may give some explanation for this effect but further analysis is required.

It would appear unlikely that we get any net electron trapping in the SiO_2 since a net negative charge in the oxide has not been observed under radiation and nonradiation environments. However, 110-keV X-ray bombardment of a similar unit prior to the proton exposure resulted in a twofold increase in drain current. There is almost no possibility of displacement damage from these photons (via Compton effect). It is clear that ionization phenomena play a significant role in the damage process.

Room temperature annealing for several days subsequent to the X-ray exposure brought the drain current approximately back down to its initial level. Several days after the proton exposure, there was a further decrease in the drain current below the final proton flux level. Little or no change in the next several months was observed. This transient decay could well have been due to the lengthened relaxation time of the vacancy annihilation process discussed earlier. There appears to be a permanent change (smaller V_P) in pinch-off voltage for this type device. High-temperature annealing studies were not made.

Figure 11 is a plot of normalized drain current versus integrated proton flux for several values of gate-source voltage of an n-channel enhancement unit. For this device there is no apparent initial increase in drain current as found in some n-channel units. But the pinch-off voltage decreases, rather rapidly leveling off near a flux of 8×10^{11} protons/cm^2. Changes in I_D past this point are very small and are probably due to degradation in carrier mobility. Apparently, the mechanism of net negative charge increase in the oxide proceeds more rapidly than the positive charge buildup from ion vacancies giving rise to the initial decrease and

subsequent saturation characteristics. This behavior along with that associated with figure 11 is presently under study.

A number of n-channel devices possessing both depletion and enhancement mode capabilities have been observed qualitatively for the two gate bias polarities during proton bombardments. Indications are that for the enhancement mode (positive gate bias) the rate of degr[illegible]tion of V_P and hence I_D is more rapid than for the depletion mode (negative gate bias) operation of the same device. The positive charge mechanism which affects device behavior supports this trend in the same manner as discussed in connection with the p-channel transistors.

Integrated Circuits

Thirteen groups of bistable multivibrators and NAND/NOR gates representing various coupling schemes (DTL, RTL, RCTL, ECL, and TTL), construction methods (triple-diffused planar and epitaxial planar), and manufacturers were evaluated. Parameters which were monitored included output logical levels, input and output leakage currents, input threshold voltages, input drive current requirements, output drive current capabilities, and transient characteristics. Transistor characteristics and parameters of other individual elements, such as resistors, were measured where accessible.

The normalized gain, β/β_O, as a function of integrated flux, is shown in figure 12 for several groups of transistors which were accessible for individual characterization. To obtain a qualitative picture of the behavior of the transistors in a radiation environment, the simplified expression for Beta is given by

$$1/\beta = X_B^2/2D_B\tau_B,$$

where: X_B = transistor base thickness
D_B = diffusion constant in the base
τ_B = minority carrier lifetime in the base region.

As shown in the above equation, Beta is proportional to minority carrier lifetime in the base region which in turn is a function of integrated flux as shown by the expression

$$1/\tau = 1/\tau_O + K\phi$$

where: τ = effective minority carrier lifetime
τ_O = initial τ
K = damage constant, dependent upon particle type, energy, and material
ϕ = integrated particle flux.

The transistor in a monolithic microcircuit differs from its conventional discrete counterpart in that it contains three junctions and four semiconductor layers, whereas the discrete transistor

contains two junctions and three semiconductor layers. The fourth layer of a monolithic device permits the existence of both NPN and PNP transistors in the same device. For instance, the substrate in a regular NPN transistor is used as the collector for the PNP transistor. This results in a low efficiency PNP device. Normalized gain of a transistor of this type used in a modified DTL NAND gate is shown in figure 12. The modification consists of the use of these low efficiency transistors in the input of the circuits in place of diodes in order to reduce the input drive current requirement and increase the fan-out capability. As shown in figure 12, these low efficiency devices are much more susceptible to radiation damage than the conventional diffused units. The greater damage in this unit was due to reduction in minority carrier lifetime in the base region (collector of the NPN transistor) and operation at very low emitter currents.[12] The degradation of gain in this instance resulted in an order of magnitude increase in drive current requirement at 2.4×10^{12} protons/cm^2. The damage to the remaining transistors was attributed to the reduction of minority carrier lifetime in the base regions.

Table II is included to show the effects of radiation on a typical RCTL NOR gate. These devices were irradiated to a total integrated flux of 1.7×10^{13} protons/cm^2. The curve in figure 12 indicates that there was a 91% loss in gain for the transistors of this circuit at 10^{13} protons/cm^2. An additional loss of 4% was recorded at 1.7×10^{13} protons/cm^2.

The output saturation voltage, $V_{CE(sat)}$, increased by 272%. This was attributed to decreased transistor gain and an increase in emitter and collector series resistance. This relationship[13] can be written as

$$V_{CE(sat)} = - \frac{kT}{q} \ln \frac{\alpha_i \left(1 - I_C/\beta I_B\right)}{1 + \left(I_C/I_B\right)(1 - \alpha_i)} + I_C r_{SC},$$

where α_i is the inverse alpha of the transistor. For a transistor with a 0.5 ohm-cm collector, α_i is approximately 0.1.

The collector series resistance, r_{SC}, can be approximated by

$$r_{SC} = \frac{\rho_c d}{2 \bar{l} X_C}$$

where: ρ_c = resistivity of the collector region
d = distance between the emitter edge and collector contact edge
X_C = thickness of collector region
$\bar{l} = 1/2(l_e + l_c)$

TABLE II. CHANGES IN PARAMETERS OF A RCTL NOR GATE DUE TO BOMBARDMENT WITH 22-MeV PROTONS TO AN INTEGRATED FLUX OF 1.7×10^{13} PROTONS/CM^2

Symbols	Parameter		Average changes, %
β	Transistor gain	$\phi_t = 1.5 \times 10^{12}$ protons/cm^2	-50
		$\phi_t = 1 \times 10^{13}$ protons/cm^2	-91
		$\phi_t = 1.7 \times 10^{13}$ protons/cm^2	-95
$V_{CE(sat)}$	Output saturation voltage		+272
$V_{min(one)}$	Input minimum Logical "one" Voltage	No load	+298
		Fan-out of 1	+296
		Fan-out of 5	+287
$V_{max(zero)}$	Input maximum Logical "zero" Voltage	No load	+184
		Fan-out of 1	+165
		Fan-out of 5	+99
I_L	Leakage Currents	Input	No significant changes
		Output	No significant changes
I_{IN}	Input drive current requirement		-4
I_{out}	Output driving current Capability	Input = 0 volt	+5 to 10
		Input = 0.5 volt	+5 to 8
V_f	Isolation diode Forward voltage		-9
R_L	Load resistor		+11
t_r	Rise time		Nonconclusive results Output pulses distorted
t_s	Storage time		
t_f	Fall time		
t_d	Delay time		

The collector series resistance in a monolithic microcircuit is greater than in its discrete counterpart due to the fact that the collector contact is made on the top surface.

In some of the devices tested, the collector series resistance was reduced by diffusion of a heavily doped region of the same polarity as the collector between the epitaxial collector and the substrate. This region has the effect of shunting the high resistivity collector region thus reducing the series collector resistance. Another advantage of this buried layer is that the resistivity of the collector region near the base can be maintained at a high level which results in low collector-base capacitance.

Considerable changes were noted in the input minimum logical "one" and input maximum logical "zero" voltages at no load and fanout of one and fanout of five. These changes reflected decreased transistor gain and increases in saturation voltage. Increases in $V_{CE(sat)}$ of one or more output transistors during irradiation can cause failure in digital microcircuits by raising the logical output voltages above the critical values selected by design.

Input and output leakage current increases were insignificant in this configuration; however, in other configurations, leakage currents increased two or three orders of magnitude. Leakage currents in silicon P-N junctions are partly attributed to the generation of charge from recombination centers within the depletion layer of the junction. Abnormally high leakage currents are most likely to be caused by charge accumulation on or within the oxide passivation leading to surface inversion layers.

The input driving current requirements, output driving current capability, isolation diode forward voltage, and load resistance changes were not considered great enough to materially affect the performance of the circuit.

The transient characteristics of the RCTL NOR gate, as indicated in table II, could not be accurately measured at an integrated flux of 1.7×10^{13} protons/cm^2 because of distortion in the output. However, at a total flux of 10^{13} protons/cm^2, no significant changes were recorded.

Figure 13 is a plot of the normalized transient characteristics as a function of integrated proton flux for an RCTL flip-flop circuit operating at a frequency of one MHZ. The time parameters, with the exception of delay time, experienced considerable changes. These parameters, primarily dependent upon output transistor characteristics, reflected a large loss in gain, β. The delay time was relatively unaffected, whereas rise and fall times increased 44% and 85%, respectively. Storage time decreased by 35%.

Rise and storage times are almost wholly dependent upon the characteristics of the output transistors as shown by the expressions[14]

$$t_r = \tau \ln \frac{1}{1 - 0.9\left(I_{CS}/\beta_f I_B\right)}$$

$$t_s = \tau \ln \tau\left(\frac{2D_B}{X_B^2} \cdot \frac{I_B}{I_{CS}}\right)$$

where: I_{CS} = saturation current
I_B = base drive current

The switching process for fall time, t_f, is similar to rise time, except the active region is traversed in the reverse direction. Loading effects are neglected in the expression for rise time but must be taken into account in an expression for fall time since the transistor represents a high impedance discharge path.

Delay time is dependent upon circuit time constants preceding the base of the output transistor and the threshold voltage of this transistor. Delay time, t_d, comes about because of the reverse bias on both emitter and collector junctions when biased to an off condition. As the effective base-emitter voltage, V_{BE}, goes from $V_{BE(off)}$ to zero, the depletion layers of both junctions must reduce in thickness. The delay time is the time required to charge the junction capacitance to the new voltage levels. These capacitances are voltage dependent and should increase during this process.

Figure 14 presents the input and output pulses of an RCTL RS flip-flop before irradiation and at integrated proton fluxes of 10^{13} protons/cm^2 and 1.7×10^{13} protons/cm^2. The circuit was triggered at a frequency of 130 KHZ with 0.5 microsecond wide pulses. The only significant change recorded at 10^{13} protons/cm^2 was a 100% increase in rise time. This could be important in applications where the output is used to drive other circuits requiring very fast rise times. At 1.7×10^{13} protons/cm^2, the circuit ceased to operate as a bistable device.

CONCLUSIONS

The results of the experimental tests have been presented for each of the three classes of electronic components discussed in this report. Conclusions derived from the results are as follows:

Junction FET's

The radiation resistance of junction FET's were found to be at least comparable to or better than most narrow-base minority carrier devices.

The zero gate transconductance of two of the three types of junction FET's studied in detail was found to vary linearly with proton flux as predicted. Unexpectedly, the zero gate drain current

of the third type also varied linearly with proton flux resulting in a nonlinear relation for transconductance.

The zero gate voltage drain current was found to have a power law relation with transconductance and the exponent ranged from 1 to 1.6 instead of the quadratic dependence predicted by the simple theory.

MOS-FET's

P-channel enhancement type MOS structures, whose characteristics depend only slightly on carrier concentration, were found to be more sensitive to radiation than most bipolar devices.

A net positive charge density in the oxide layer observed in all p-channel and some n-channel devices is believed to be due to positively charged oxygen-ion vacancies created through collisions with the energetic particles.

In p-channel enhancement devices, the net oxide charge causes the pinch-off voltage to take on successively more negative values, thus degrading the drain current and transconductance.

For some n-channel enhancement-depletion devices, the same negative increase in V_p occurs at early stages of bombardment. The pinch-off voltage then reaches a maximum and begins to move toward zero indicating either an increasing density of negative charge in the oxide or on the surface. Finally, other n-channel transistors showed no tendency for a negative increase in V_p but rather toward zero. The causes for the n-channel behavior are not clearly understood at this time.

Integrated Circuits

No particular type of construction, coupling scheme, or manufacturer's device was found to be highly superior to another in resistance to 22-MeV proton irradiation.

The predominant cause of failure was found to be the degradation in transistor gain, which affects the performance of the microcircuits in numerous ways depending upon the particular circuit configuration. Therefore, the use of transistors with the highest frequency response (narrowest base) practical for the application is recommended.

Rise time increased and storage time decreased with radiation. Delay time and fall time increased with radiation in most instances.

REFERENCES

1. Floyd R. Bryant and Carl L. Fales, "Damage to Field-Effect Transistors Under 22- and 126-MeV Proton Bombardments", NASA TN D-3630 (1966).

2. J. E. Drennan and D. J. Hamman, "Report on Space-Radiation Damage to Electronic Components and Materials", REIC Report No. 39 (January 31, 1966).

3. W. Shockley, "A Unipolar Field-Effect Transistor", Proc. I.R.E., Vol. 40, pp 1365-1376 (November, 1952).

4. I. Richer and R. D. Middlebrook, "Power-Law Nature of Field-Effect Transistor Experimental Characteristics", Proc. I.E.E.E., Vol. 51, pp 1145-1146 (August, 1963).

5. R. D. Middlebrook, "A Simple Derivation of Field-Effect Transistor Characteristics", Proc. I.E.E.E., Vol. 51, pp 1145-1147 (August, 1963).

6. G. K. Wertheim, "Energy Levels in Electron-Bombarded Silicon", Phys. Rev., Vol. 105, No. 6, pp 1730-1735 (March 15, 1957).

7. R. A. Breckenridge and C. Gross, "Damage to Germanium Due to 22- and 40-MeV Proton Bombardment", NASA TN D-2727 (1965).

8. R. A. Breckenridge and C. Gross, "Private Communication".

9. G. C. Messenger, et al., "Displacement Damage in MOS Transistors", Proc. I.E.E.E., Trans. Nuclear Science, Vol. NS-12, No. 5 (October, 1965).

10. J. E. Thomas and D. R. Young, "Space-Charge Model for Surface Potential Shifts in Silicon Passivated With Thin Insulating Layers", IBM Journal of Research and Development, Vol. 8, No. 4 (September, 1964).

11. S. R. Hofstein and F. P. Heiman, "The Silicon Insulated Gate Field-Effect Transistor", Proc. I.R.E., Vol. 51, pp 1190-1202 (September, 1963).

12. Transistor Design Effects on Radiation Resistance, Final Report, Contract No. NAS1-4595 (1965).

13. R. M. Warner, ed., "Integrated Circuits, Design Principles and Fabrication", McGraw-Hill Book Co., Inc. (1965).

14. A Study of the Effect of Space Radiation on Silicon Integrated Microcircuits, Final Report, Contract No. NAS5-3985 (1965).

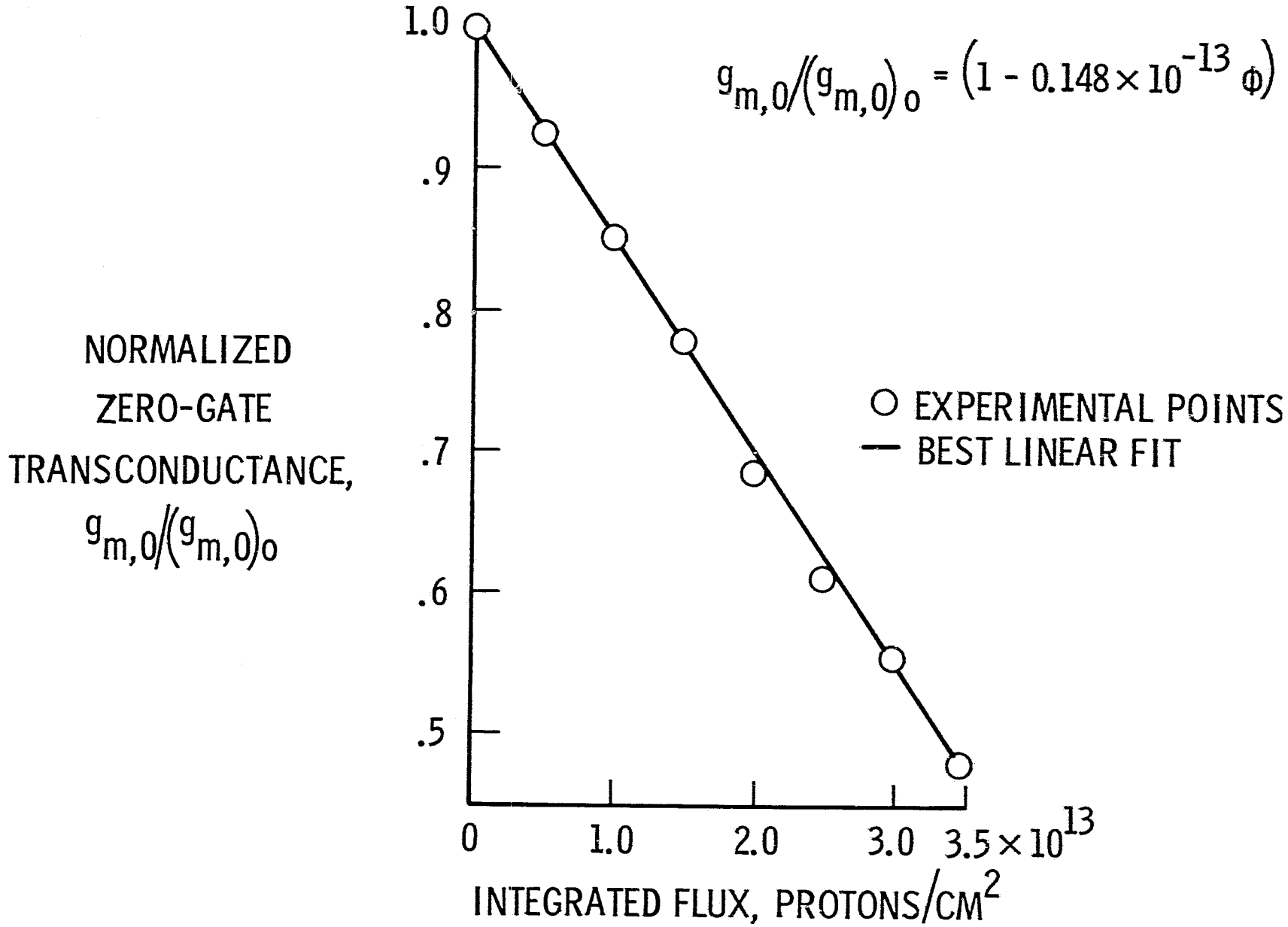

FIGURE 1.- NORMALIZED ZERO-GATE TRANSCONDUCTANCE AS A FUNCTION OF 22-MeV PROTON FLUX FOR TRANSISTOR TYPE 2N3070 (n-CHANNEL).

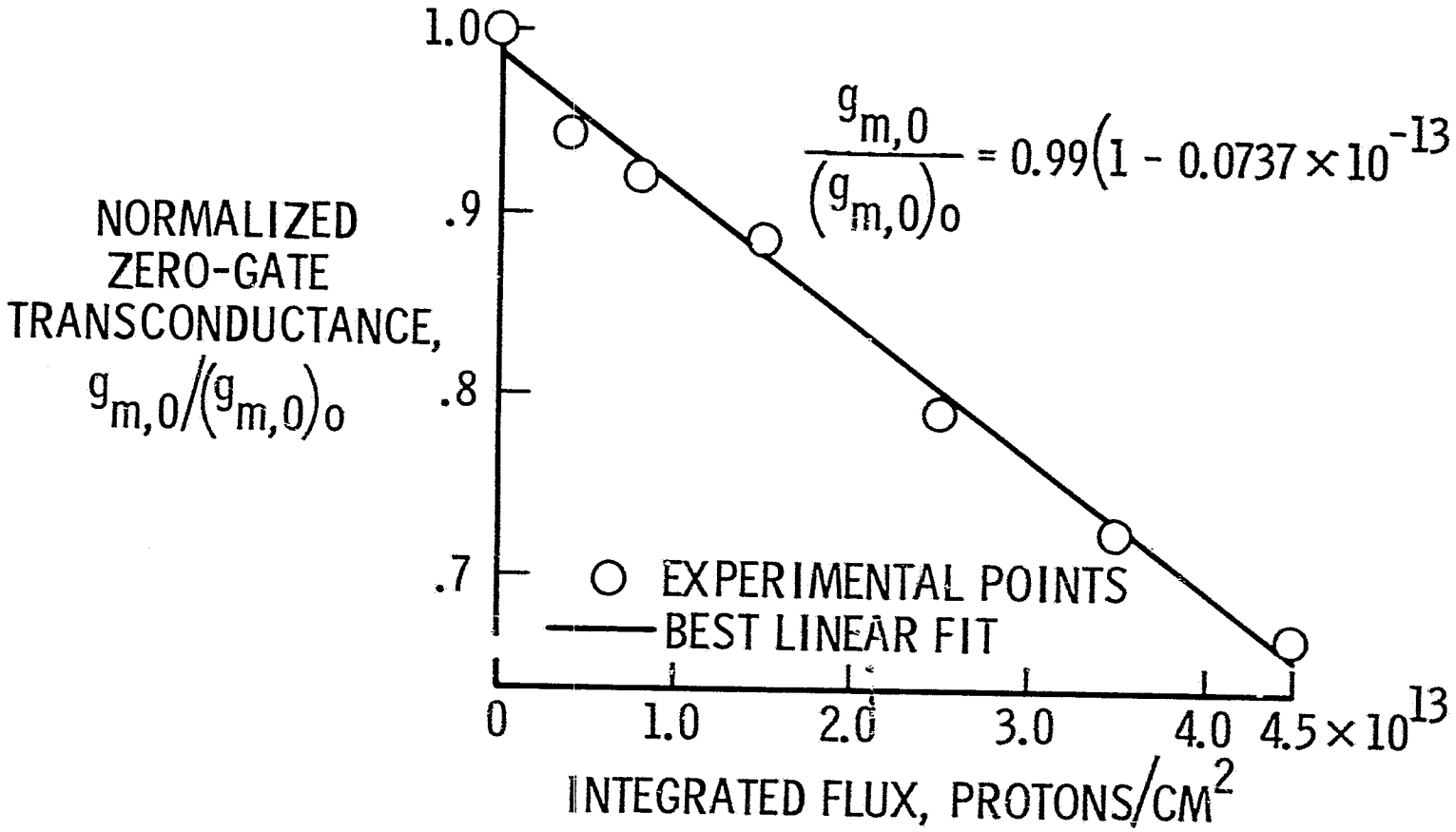

FIGURE 2.- NORMALIZED ZERO-GATE TRANSCONDUCTANCE AS A FUNCTION OF 22-MeV PROTON FLUX FOR TRANSISTOR TYPE 2N2844 (p-CHANNEL).

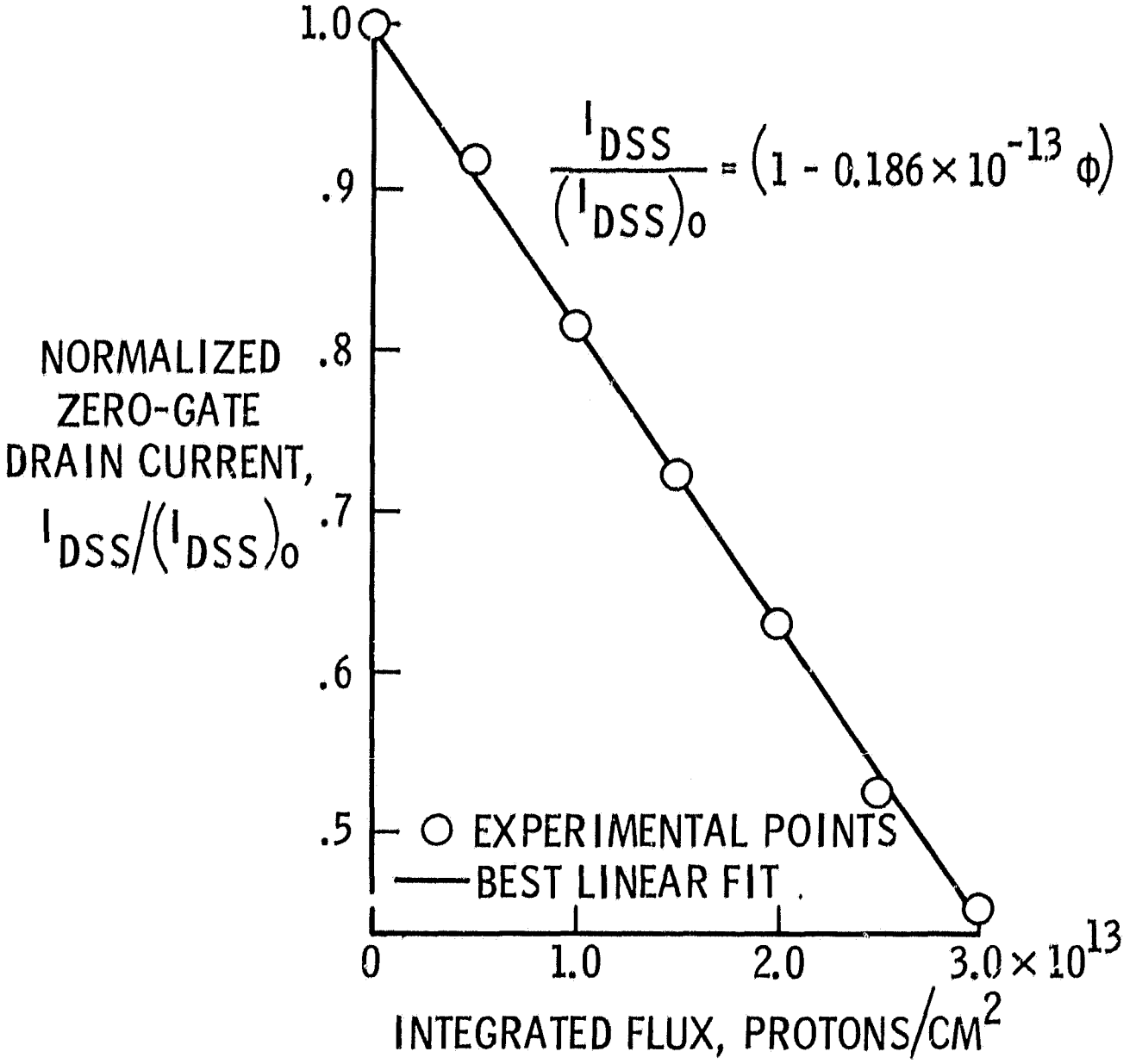

FIGURE 3.- NORMALIZED ZERO-GATE DRAIN CURRENT AS A FUNCTION OF 22-MeV PROTON FLUX FOR TRANSISTOR TYPE 2N3067 (n-CHANNEL).

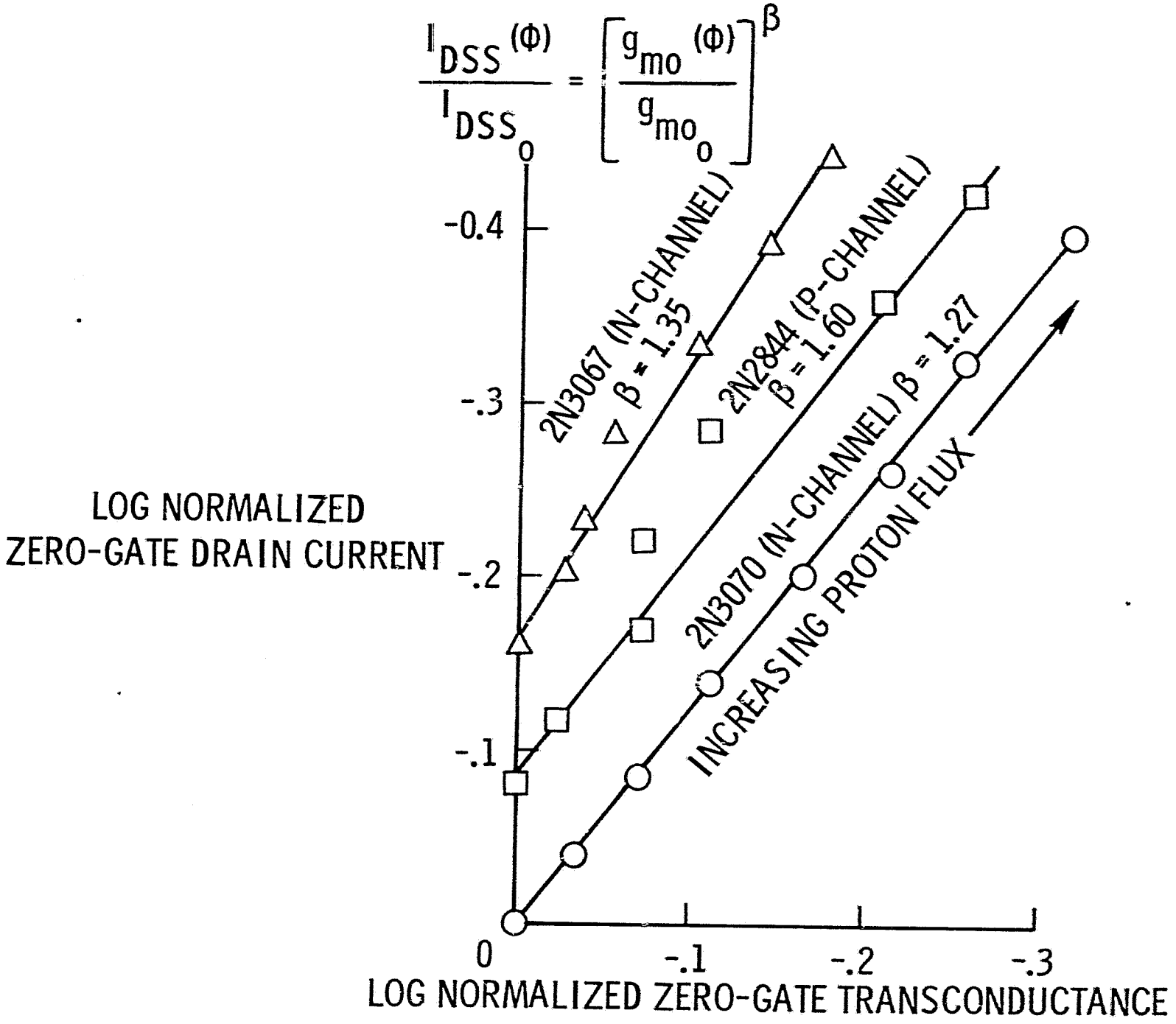

FIGURE 4.- LOG NORMALIZED ZERO-GATE DRAIN CURRENT AS A FUNCTION OF LOG NORMALIZED ZERO-GATE TRANSCONDUCTANCE FOR 22-MeV PROTON BOMBARDMENT.

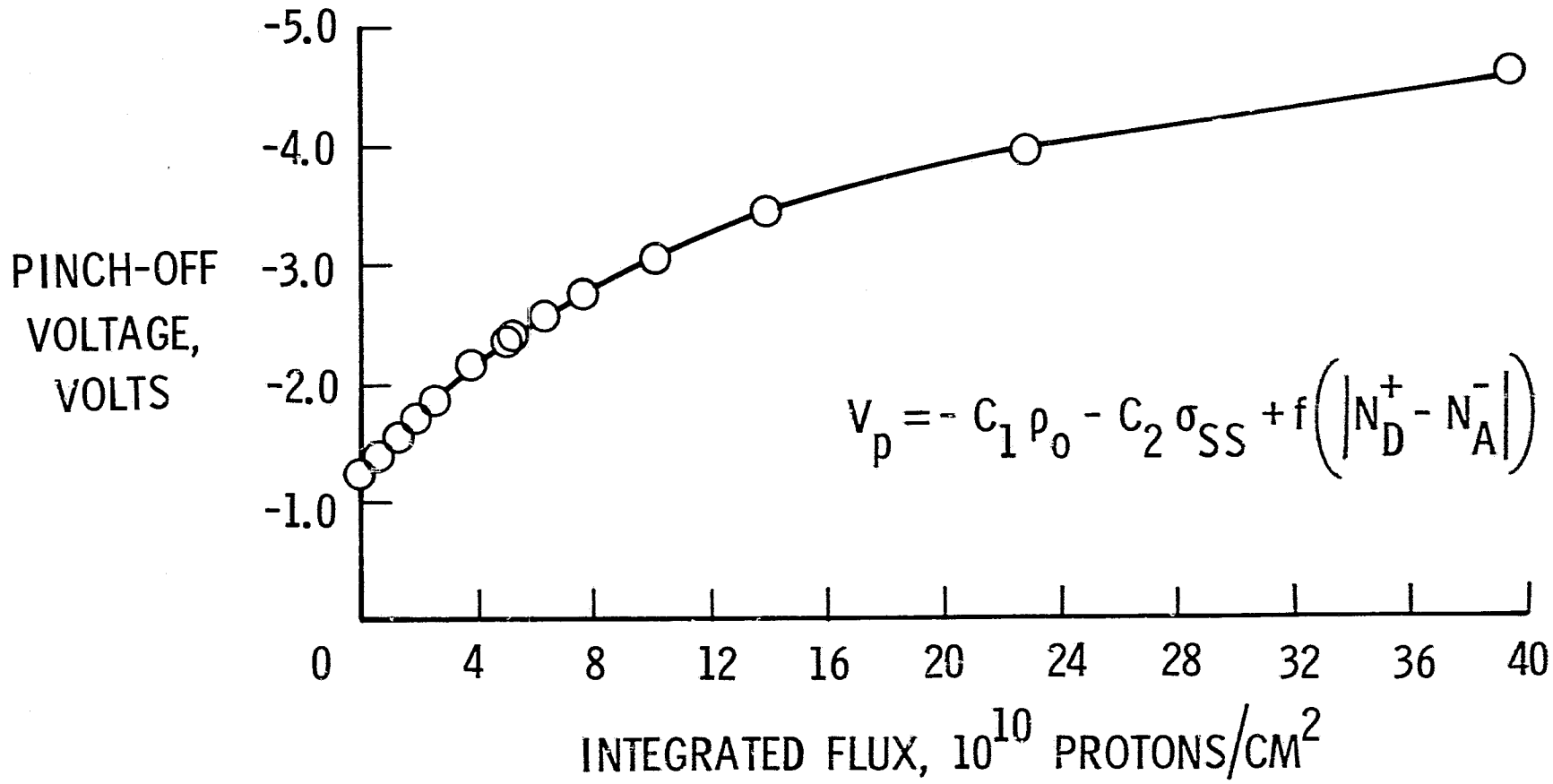

FIGURE 5.- PINCH-OFF VOLTAGE AS A FUNCTION OF INTEGRATED PROTON (22 MeV) FLUX FOR p-CHANNEL ENHANCEMENT MOS-FET.

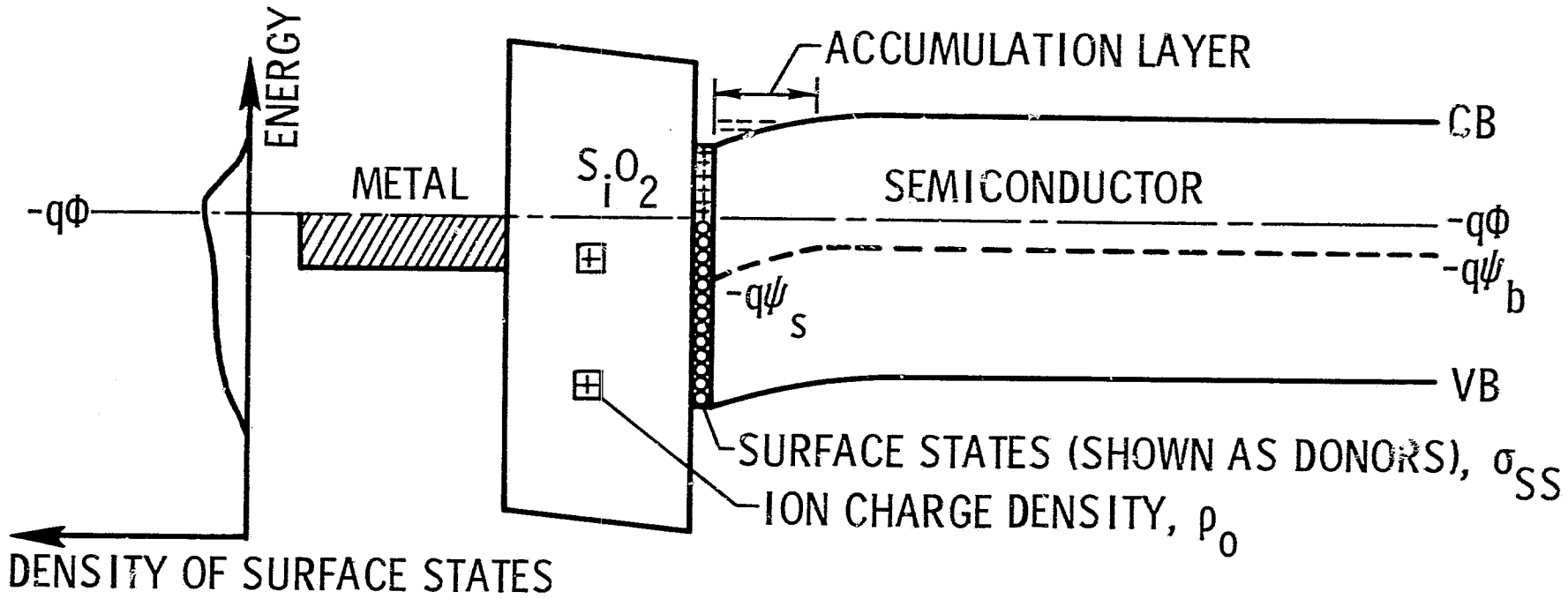

FIGURE 6.- BAND DIAGRAM OF MOS STRUCTURE BEFORE IRRADIATION.

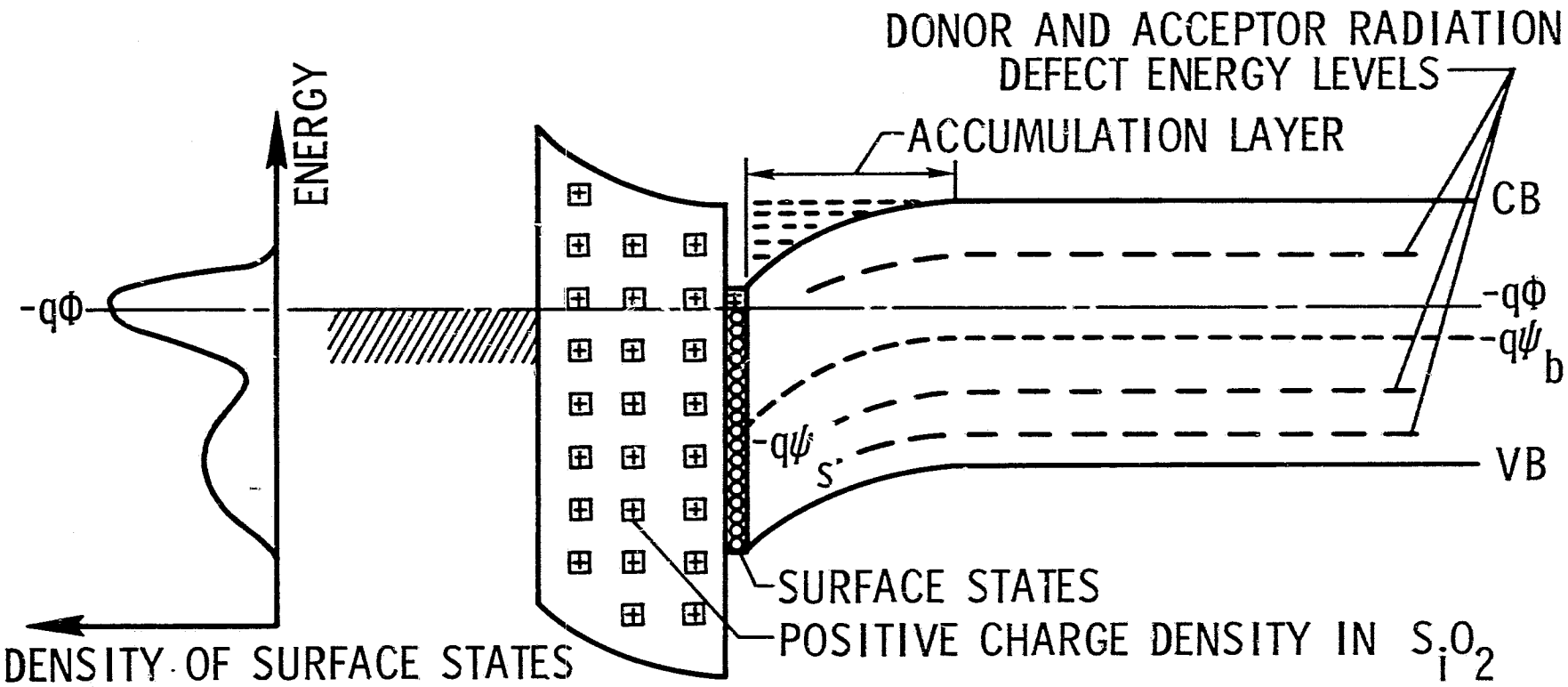

FIGURE 7.- BAND DIAGRAM OF MOS STRUCTURE AFTER IRRADIATION.

$$I_D = - C\mu_p \left(V_{GS} - V_p\right)^2$$

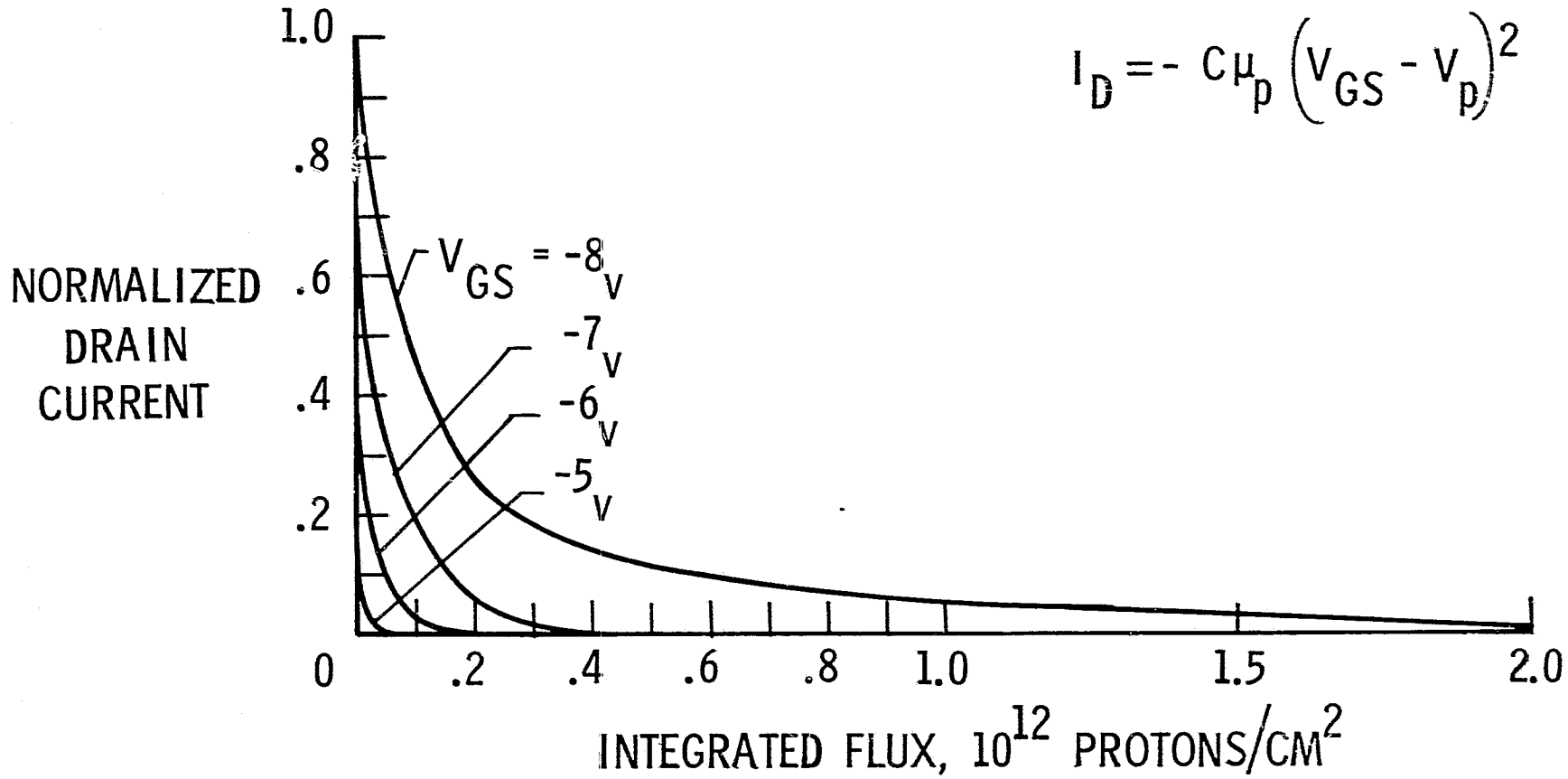

FIGURE 8.- NORMALIZED DRAIN CURRENT AS A FUNCTION OF INTEGRATED PROTON (22 MeV) FLUX FOR p-CHANNEL ENHANCEMENT MOS-FET, WHERE I_o = 7.6 ma AND V_{DS} = -5V.

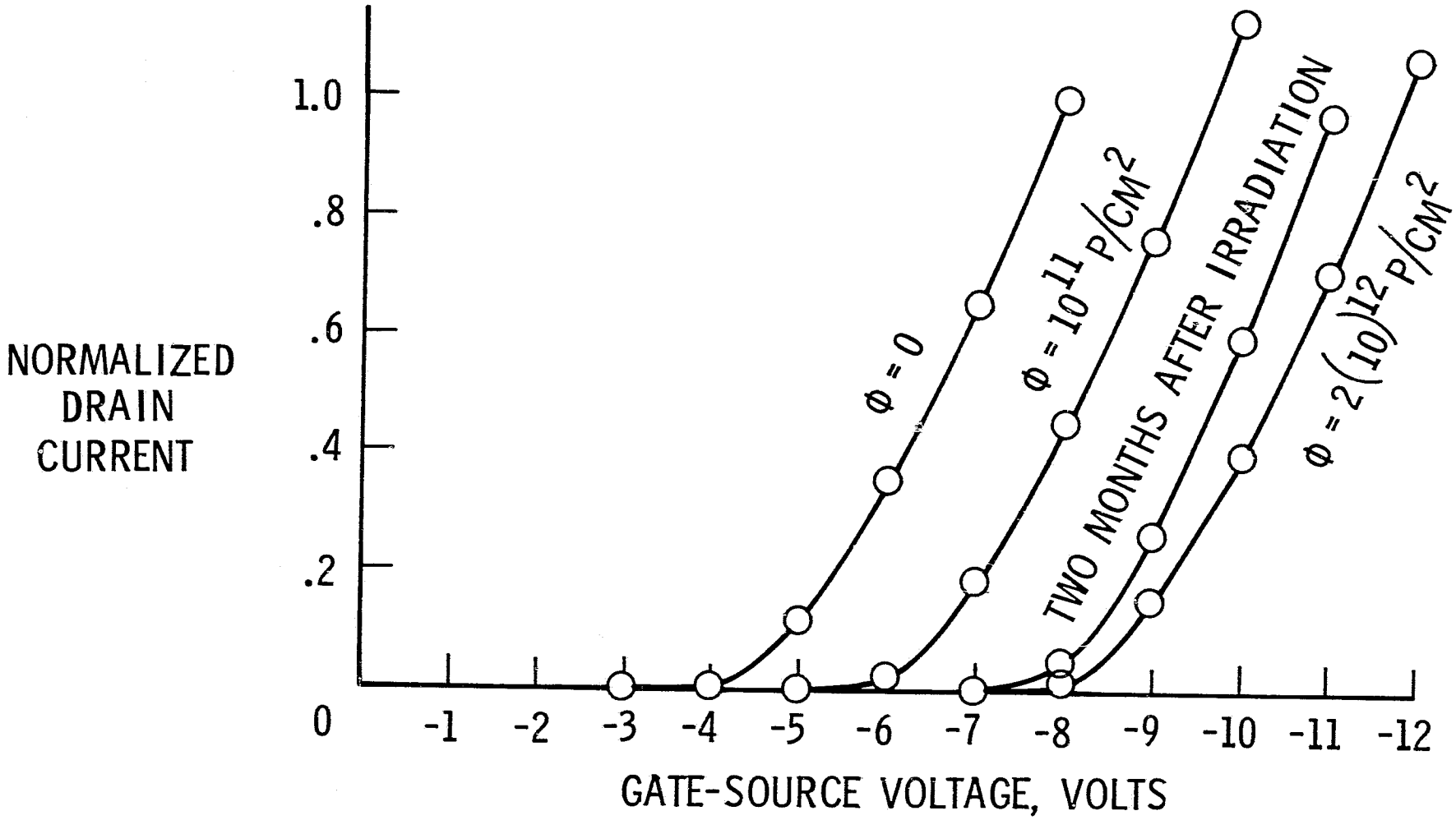

FIGURE 9.- NORMALIZED DRAIN CURRENT AS A FUNCTION OF GATE-SOURCE VOLTAGE (22-MeV PROTONS) FOR p-CHANNEL ENHANCEMENT MOS-FET, WHERE I_O = 7.6 ma AND V_{DS} = -5V.

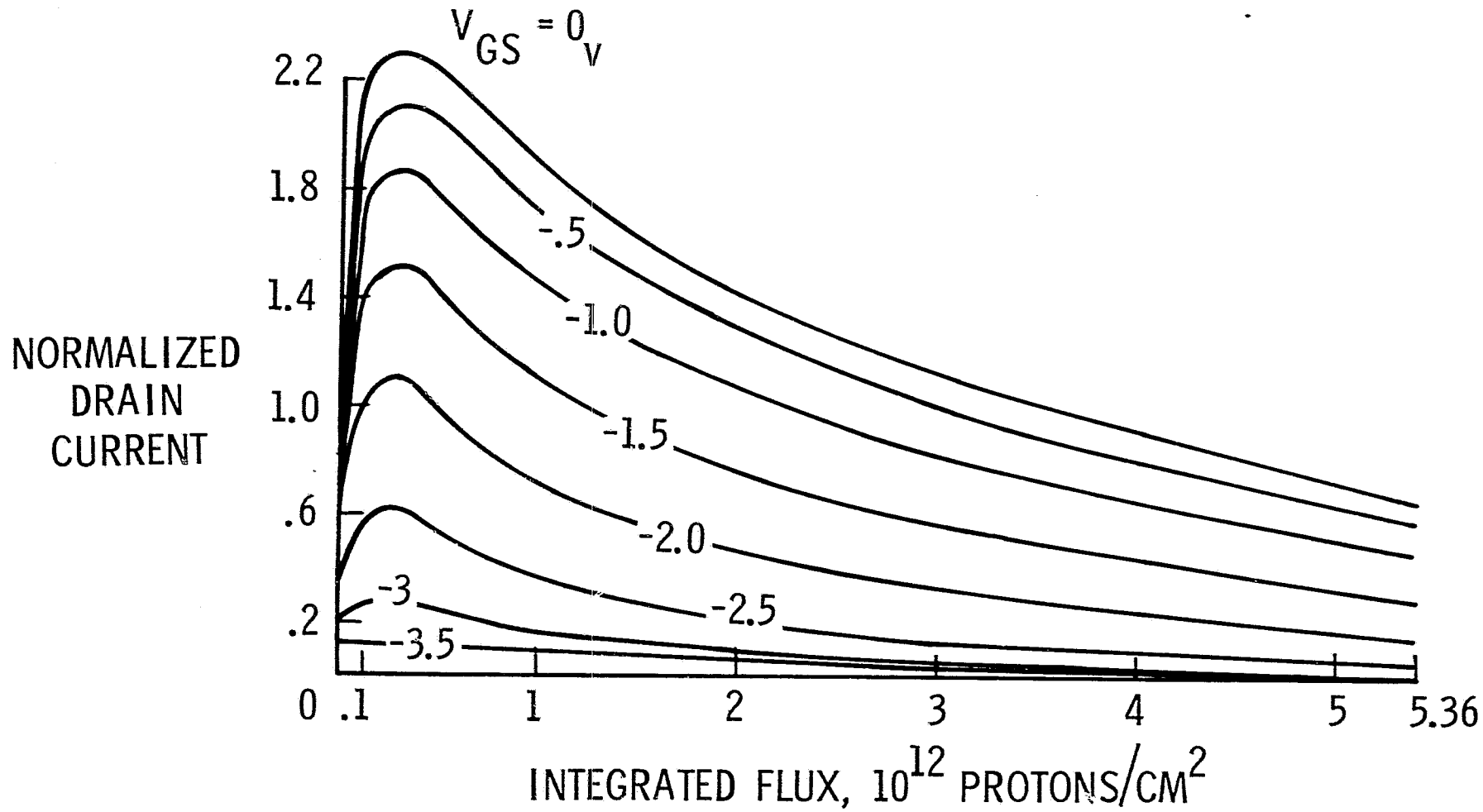

FIGURE 10.- NORMALIZED DRAIN CURRENT AS A FUNCTION OF INTEGRATED PROTON (22 MeV) FLUX FOR n-CHANNEL DEPLETION MOS-FET, WHERE I_o = 3.1 ma AND V_{DS} = -5V.

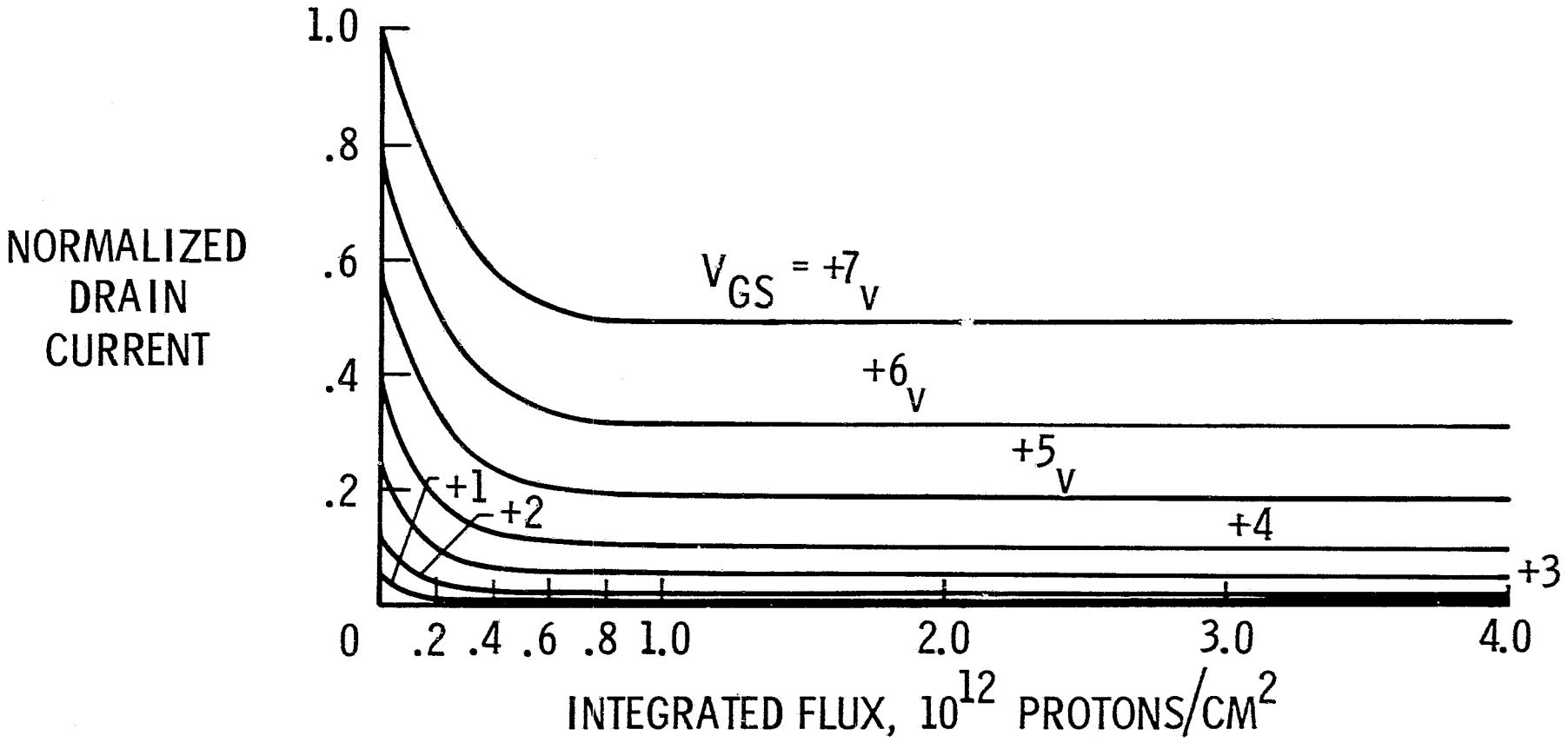

FIGURE 11.- NORMALIZED DRAIN CURRENT AS A FUNCTION OF INTEGRATED PROTON (22 MeV) FLUX FOR n-CHANNEL ENHANCEMENT MOS-FET, WHERE I_o = 1.86 ma AND V_{DS} = +7V.

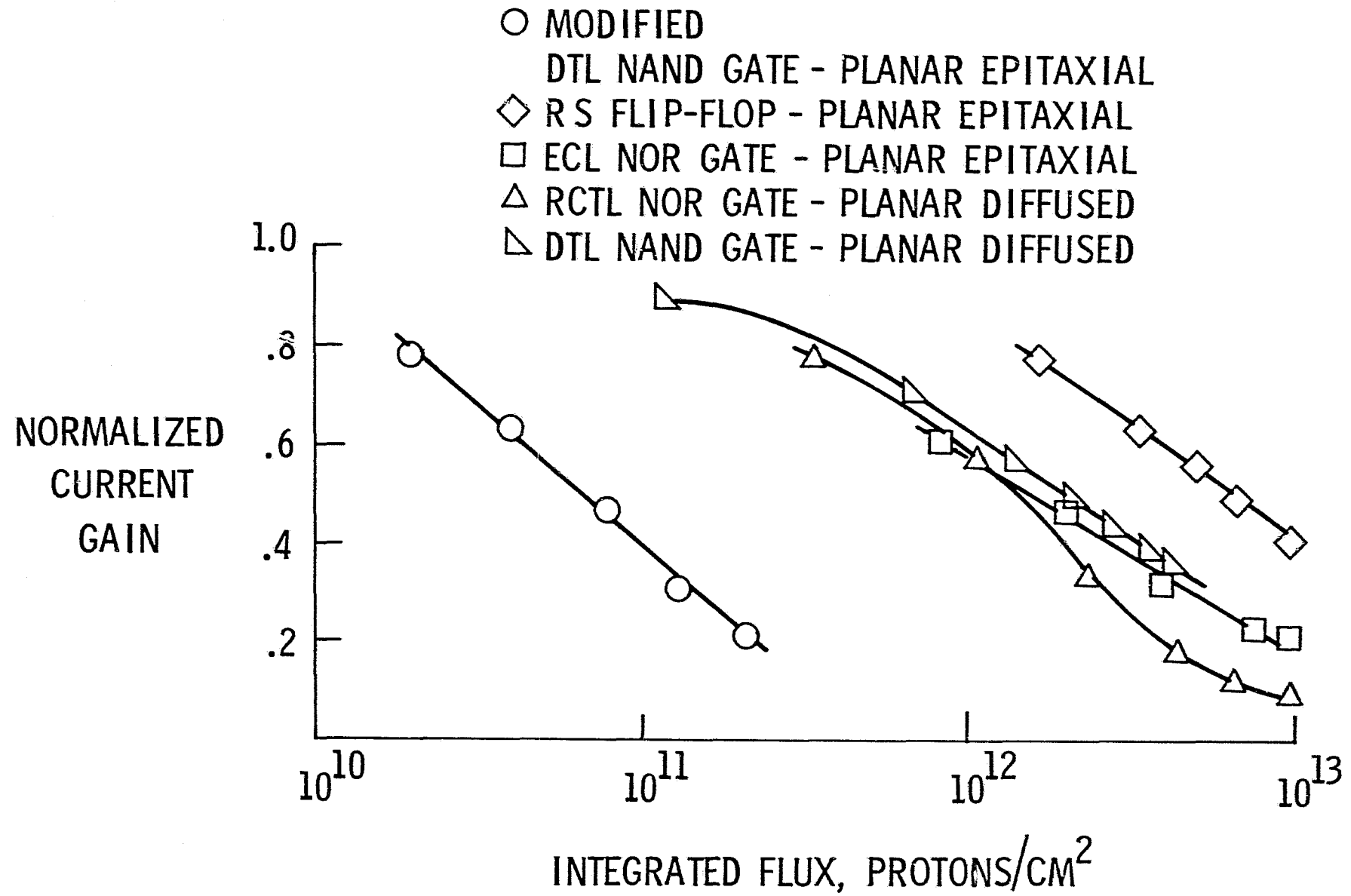

FIGURE 12.- NORMALIZED COMMON EMITTER CURRENT GAIN AS A FUNCTION OF INTEGRATED PROTON (22 MeV) FLUX FOR VARIOUS INTEGRATED CIRCUIT TRANSISTORS.

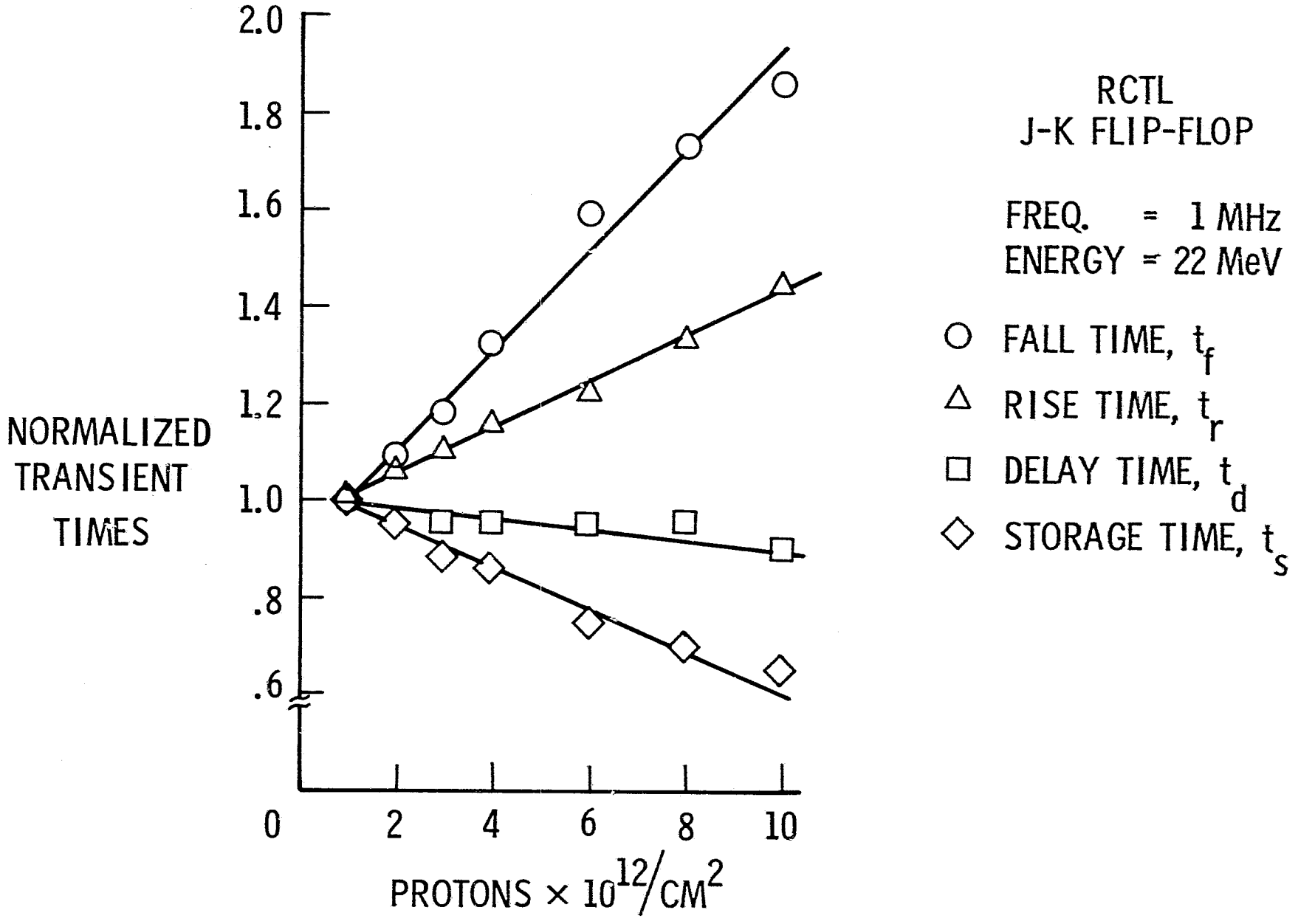

FIGURE 13.- NORMALIZED TRANSIENT CHARACTERISTICS AS A FUNCTION OF INTEGRATED PROTON FLUX.

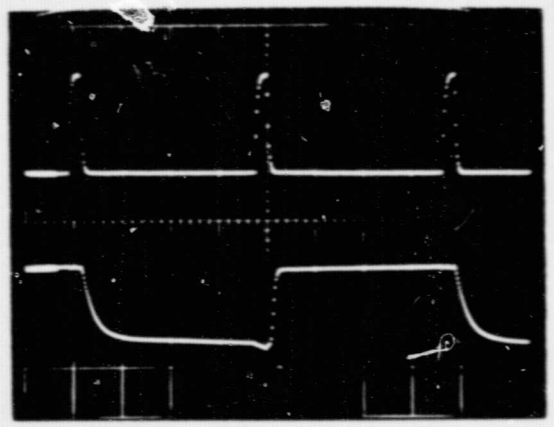

$\Phi_t = 0$

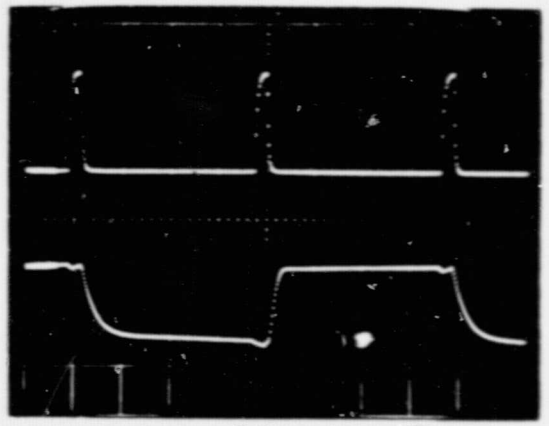

$\Phi_t = 10^{13}$ P/CM^2

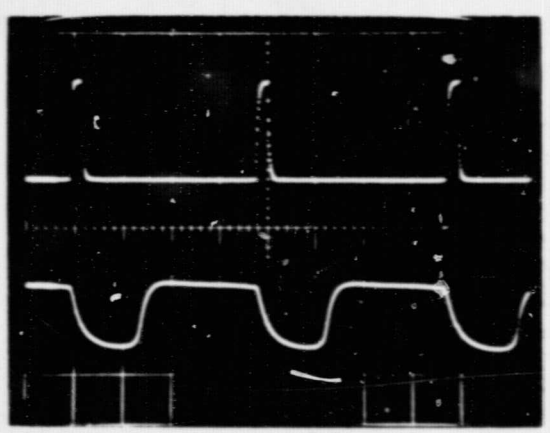

$\Phi_t = 1.7 \times 10^{13}$ P/CM^2

SCALE:

HORIZONTAL

2.25 μSEC/DIV.

VERTICAL

TOP TRACE - 1.0 VOLT/DIV.
BOTTOM TRACE - 2.0 VOLTS/DIV.

FIGURE 14.- RCTL RS FLIP-FLOP OUTPUT BEFORE AND AFTER BOMBARDMENT WITH 22-MeV PROTONS.

NASA-Langley, 1966